Optimal Te-doping in GaSe for non-linear applications

Shin An Ku,[1] Wei-Chen Chu,[1] Chih Wei Luo,[1,*] Yu. M. Andreev,[2] Grigory Lanskii,[2] Anna Shaidukoi,[2] Tatyana Izaak,[3] Valery Svetlichnyi,[3] Kaung Hsiung Wu,[1] and T. Kobayashi[1,4]

[1] *Department of Electrophysics, National Chiao-Tung University, Hsinchu, Taiwan*
[2] *Institute of Monitoring of Climatic and Ecological Systems of Siberian Branch of Russian Academy of Sciences, Tomsk, Russia*
[3] *Siberian Physical-Technical Institute of Tomsk State University, 1 Novosobornaya Sq., Tomsk, Russia*
[4] *Advanced Ultrafast Laser Research Center, and Department of Engineering Science, Faculty of Informatics and Engineering, The University of Electro-Communications, Chofugaoka 1-5-1, Chofu, Tokyo 182-8585 Japan*

[*] *cwluo@mail.nctu.edu.tw*

Abstract: Centimeter-sized Te-doped GaSe ingots were grown from the charge compositions of GaSe with nominals 0.05, 0.1, 0.5, 1, and 3 mass% Te, which were identified as ε-GaSe:Te (0.01, 0.07, 0.38, 0.67, and 2.07 mass%) single crystals. The evolution of the absorption peaks of the phonon modes E'$^{(2)}$ ($\sim$0.584 THz) and E''$^{(2)}$ (1.77 THz) on Te-doping in GaSe:Te crystals was studied by THz time-domain spectroscopy. This study proposes that the evolution of both E'$^{(2)}$ and E''$^{(2)}$ absorption peaks correlates well with the optical quality of Te-doped GaSe crystals, which was confirmed by experimental results on the efficiency of THz generation by optical rectification. Maximal intensity of the absorption peak of the rigid layer mode E'$^{(2)}$ is proposed as a criterion for identification of optimal Te-doping in GaSe crystals.

© 2012 Optical Society of America

OCIS codes: (320. 7150) Ultrafast spectroscopy; (190.4400) Nonlinear optics, materials.

References and links

1. V. G. Dmitriev, G. G. Gurzadyan, and D. N. Nikogosyan, *Handbook of Nonlinear Optical Crystals*, (Springer, Berlin, 1997), pp. 166-169.
2. R. Huber, A. Brodschelm, F. Tauser, and A. Leitenstorfer, "Generation and field-resolved detection of femtosecond electromagnetic pulses tunable up to 41 THz," Appl. Phys. Lett. **76,** 3191–3193 (2000).
3. N. C. Fernelius, "Properties of gallium selenide single crystal," Prog. Cryst. Growth Charact. **28,** 275–353 (1994).
4. W. Y. Liang, "Optical anisotropy in GaSe," J. Phys. C: Solid State Phys. **8,** 1769–1768 (1975).
5. R. Le Toullec, N. Piccioli, M. Mejatty, and M. Balkanski, "Optical constants of ε-GaSe," Nuovo Cimento **38B,** 159–167 (1977).
6. A. A. Tikhomirov, Yu. M. Andreev, G. V. Lanskii, O. V. Voevodina, and S. Yu. Sarkisov, "Doped GaSe nonlinear crystals," Proc. SPIE. **6258,** 64–72 (2006).
7. K. R. Allakhverdiev, R. I. Guliev, E. Yu. Salaev, and V. V. Smirnov, "An investigation of linear and nonlinear optical properties of GaS_xSe_{1-x} crystals," Sov. J. Quantum Electron. **12,** 947–949 (1982).
8. D. R. Suhre, N. B. Singh, V. Balakrishna, N. C. Fernelius, and F. K. Hopkins, "Improved crystal quality and harmonic generation in GaSe doped with indium," Opt. Lett. **22,** 775–777 (1997).
9. N. B. Singh, D. R. Suhre, W. Rosch, R. Meyer, M. Marable, N. C. Fernelius, F. K. Hopkins, D. E. Zelmon, and R. Narayanan, "Modified GaSe crystals for mid-IR applications," J. Cryst. Growth **198,** 588–592 (1999).
10. Y. -K. Hsu, C. -W. Chen, J. Y. Huang, C. -L. Pan, J. -Y. Zhang, and C. -S. Chang, "Erbium doped GaSe crystal for mid-IR applications," Opt. Express **14,** 5484–5491 (2006).

#157970 - $15.00 USD Received 10 Nov 2011; revised 16 Dec 2011; accepted 6 Jan 2012; published 14 Feb 2012

11. Z. -S. Feng, Z. -H. Kang, F. -G. Wu, J. -Y. Gao, Y. Jiang, H. -Z. Zhang, Y. M. Andreev, G. V. Lanskii, V. V. Atuchin, and T. A. Gavrilova, "SHG in doped GaSe:In crystals," Opt. Express **16,** 9978–9985 (2008).
12. Y. -F. Zhang, R. Wang, Z. -H. Kang, L. -L. Qu, Y. Jiang, J. -Y. Gao, Y. M. Andreev, G. V. Lanskii, K. Kokh, A. N. Morozov, A. V. Shaiduko, E. Vinnik, and V. V. Zuev, "$AgGaS_2$- and Al-doped GaSe for IR Application," Opt. Commun. **284,** 1677–1681 (2011).
13. Z. Rak, S. D. Mahanti, K. C. Mandal, and N. C. Fernelius, "Doping dependence of electronic and mechanical properties of $GaSe_{1-x}Te_x$ and $Ga_{1-x}In_xS$ e from first principles," Phys. Rev. B **82,** 155203-1-10 (2010).
14. Y. J. Ding and W. Shi, "Widely tunable monochromatic THz sources based on phase-matched difference-frequency generation in nonlinear-optical crystals: A novel approach," Laser Phys. **16,** 562–570 (2006).
15. C. -W. Chen, T. -T. Tang, S. -H. Lin, J. Y. Huang, C. -S. Chang, P. -K. Chung, S. -T. Yen, and C. -L. Pan, "Optical properties and potential applications of ε-GaSe at terahertz frequencies," J. Opt. Soc. Am. B **26,** A58–A65 (2009).
16. Z. -W. Luo, X. -A. Gu, W. -C. Zhu, W. -C. Tang, Y. M. Andreev, G. Lanskii, A. Morozov, and V. Zuev, "Optical properties of GaSe:S crystals in terahertz frequency range," Opt. Precision Eng. (in Chinese) **19,** 354–359 (2011).
17. K. C. Mandal, S. H. Kang, M. Choi, J. Chen, X. -C. Zhang, J. M. Schleicher, C. A. Schmuttenmaer, and N. C. Fernelius, "III-VI Chalcogenide semiconductor crystals for broadband tunable THz sources and sensors," IEEE J. Sel. Top. Quant. Electron **14,** 284–288 (2008).
18. C.-W. Chen, Y-K. Hsu, J. Y. Huang, C.-S. Chang, J.-Y. Zhang, and C.-L. Pan, "Generation properties of coherent infrared radiation in the optical absorption region of GaSe crystal," Opt. Express **14,** 10636–10644 (2006).
19. S. Y. Sarkisov, V. V. Atuchin, T. A. Gavrilova, V. N. Kruchinin, S. A. Bereznaya, Z. V. Korotchenko, O. P. Tolbanov, and A. I. Chernyshev, "Growth and optical parameters of GaSe:Te crystals," Russ. Phys. J. **53,** 346–352 (2010).
20. G. B. Abdullaev, K. R. Allakhverdiev, S. S. Babaev, E. Yu. Salaev, M. M. Tagyev, L. K. Vodopyanov, and L. V. Golubev, "Raman scattering from $GaSe_{1-x}Te_x$," Solid State Commun. **34,** 125–128 (1980).
21. B. L. Yu, F. Zeng, V. Kartazayev, R. R. Alfano, and K. C. Mandal, "Terahertz studies of the dielectric response and second-order phonons in a GaSe crystal," Appl. Phys. Lett. **87,** 182104-1-3 (2005).
22. H. Yoshida, S. Nakashima, and A. Mitsuishi, "Phonon Raman spectra of layer compound GaSe," Phys. Status Solidi B **59,** 655–666 (1973).
23. I. Evtodiev, L. Leontie, M. Caraman, M. Stamate, and E. Arama, "Optical properties of p-GaSe single crystals doped with Te," J. App. Phys. **105,** 023524-1-5 (2009).
24. G. M. Mamedov, M. Karabulut, H. Ertap, O. Kodolbas, O. Oktu, and A. Bacoglu, "Exciton photoluminescence, photoconductivity and absorption in $GaSe_{0.9}Te_{0.1}$ alloy crystals," J. Lumin. **129,** 226–230 (2009).
25. E. A. Meneses, N. Jannuzzi, J. R. Freitas, and A. Gouskov, "Photoluminescence of layered GaSe1-xTex crystals," Phys. Stat. Sol. (b) **78,** K35–K38 (1976).
26. S. Shigetomi and T. Ikari, "Optical and electrical characteristics of p-GaSe doped with Te," J. Appl. Phys. **95,** 6480–6482 (2004).

1. Introduction

The optical properties of GaSe have been successfully used to generate coherent radiation in the mid-infrared and down to the terahertz (THz) frequency range [1,2]. Several unique properties of GaSe are associated with its layered structure. The basic four-fold layer consists of two monoatomic sheets of Ga sandwiched between two monoatomic sheets of Se. The strong covalent interaction within these basic layers and the Van-der-Waals-type weak bonding between these basic layers renders GaSe a highly anisotropic material. GaSe crystals are negative uniaxial crystals and belong to the point group of $\bar{6}2m$. Four polymorphic modifications were identified in the GaSe compound. The atom arrangement in one layer is the same for all four modifications; however, layer stacking can be classified by the noncentrosymmetric δ, ε, and γ or the centrosymmetric β modifications [3]. In general, GaSe crystals grown by the conventional Bridgeman technique are ε-polytype. Because of the layer structure, GaSe crystals exhibit considerable anisotropic absorption at short-wavelength edges of visible and THz ranges, and at long-wavelength edge of mid-IR range. The strongly anisotropic absorption ($\alpha_e > \alpha_o$) at short-wavelength visible range is related to anisotropic band structure and the selection rules for the optical absorption in layered GaSe crystals [4,5]. Additionally, the layer structure of GaSe results in low (almost zero by Mohs scale) hardness, and the crystals can be easily cleaved along planes parallel with the atomic layers, which hamper large-area applications.

GaSe is an excellent matrix material for doping with various elements. An original ε-polytype structure of GaSe was strengthened by doping; the physical properties responsible for

the frequency conversion efficiency were also modified [6–13]. Although the THz generation and optical properities in GaSe have been examined in detail [2, 14, 15], few studies focused on the optical properties in THz range and the THz generation by doped GaSe crystals. The optical properties were studied experimentally in S-doped GaSe (GaSe:S) [16], GaSe:In [17], GaSe:Er [10, 18], GaSe:Al [12], and GaSe:Te [17, 19, 20]. This indicates that the optical properties and THz gerneation effecicency of GaSe are strongly doping dependent. However, no systematical studies were conducted to find the optimally doped GaSe-based system for both mid-IR and THz applications. To our knowledge, no simple and reliable methods can be applied to identify the optimal doping in GaSe crystals for THz applications.

Among the physical properities, the far-infrared absorption of a non-linear crystal is a practical limitation on the optical rectification and down conversion. The far infrared absorption of a crystal is usually attributed to infrared-active phonon modes or their combination modes. For instance, Chen et al. [15] experimentally studied the effect of phonon mode of rigid layer mode $E'^{(2)}$ centered at 0.596 THz on the refractive index and THz generation efficiency in GaSe. In addition, the phonon mode of $E''^{(2)}$ at 1.78 THz was found in GaSe:S crystals [16], which demonstrated that the doping of S suppressed the rigid layer mode $E'^{(2)}$ and caused the $E''^{(2)}$ mode. However, the doping-dependent evolution between two modes of $E'^{(2)}$ and $E''^{(2)}$ remains unclear.

This paper reports the growth of centimeter-sized ingots with ε-GaSe:Te (nominal 0.05, 0.1, 0.5, 1, and 3 mass% in the charge composition) single crystals for non-linear applications. The strong correlation between the structure and the phonon modes in various Te-doped GaSe crystals was observed for the first time by measuring the absorption spectra in mm-long samples. As Te concentration increased, the absorption peak of rigid layer mode $E'^{(2)}$ markedly rose and subsequently shrunk with the simultaneous appearance of phonon mode $E''^{(2)}$ at 1.77 THz in heavy Te-doping. This study also proposed that the evolution of $E'^{(2)}$ and $E''^{(2)}$ modes can be used to identify the lattice structure and the optical quality in Te-doped GaSe crystals, which was experimentally confirmed by the study of THz generation efficiency at various Te-doping levels. The THz generation efficiency from $\sim$0.3-mm-thick Te-doped samples with 0.07 mass% was over 20% higher than that in a pure GaSe crystal with same thickness, and was consistent with the highest absorption peak of the rigid layer mode $E'^{(2)}$. Finally, the doping-dependent evolution of the rigid layer mode $E'^{(2)}$ may be used as a criterion for identifying the optimal doping in GaSe or other crystals.

2. Crystal growth and characterization

2.1. Growth technology

The GaSe:Te crystals were prepared according to the following processes. Initially, the polycrystalline materials with 120-150 g were synthesized in a two-zone horizontal furnace by using high purity (99.9999%) gallium (Ga), selenium (Se), and 99.9% tellurium (Te). The synthesis was performed in sealed quartz ampoules, which were evacuated to 10^{-5} Torr. Weighted charges of Ga and Se were placed in the boats located at hot and cold ends of the ampoule. A GaSe crystal was synthesized through three sequential stages with different temperature profiles over the ampoule, as described elsewhere [11]. Chemical reaction of the reagents up to GaSe formation was produced in the first stage by interacting between the vapor from the sublimation of Se at 690°C and Ga melt at 970°C; that is, the GaSe compound was synthesized in the reaction ampoule under selenium vapor pressure. In the second stage, the melt further homogenized at 1000°C through diffusion. In the final stage, the melt was cooled for 36 hours to form a large block and homogeneous GaSe ingot. For GaSe:Te crystals, Te with 0.05, 0.1, 0.5, 1, and 3 mass% were added into the boat with gallium during synthesis. The temperature gradient at the crystallization front was 10°C/cm, and the crystal pulling rate was 10 mm/day.

#157970 - $15.00 USD Received 10 Nov 2011; revised 16 Dec 2011; accepted 6 Jan 2012; published 14 Feb 2012
(C) 2012 OSA

Figure 1 shows the typical microscopic image of the pure and Te-doped GaSe single crystals.

The concentration of Te in GaSe:Te crystals was determined as 0.01, 0.07, 0.38, 0.67, and 2.07 mass% by electron probe micro-analyzer (EPMA, JEOL JXA-8800M). In addition, the EPMA results show the homogenous distribution of Te in all of the samples used in this study. The crystal structures of all samples were recognized as the ε-polytype of $\bar{6}2m$ point group by the X-ray diffraction patterns. The samples were prepared by cleaving the middle part with most homogeneity of an as-grown ingot parallel to the z-cut layer, and were used without additional treatment. The same samples or their parts were also used in various studies of this work. Additionally, the microhardness of GaSe:Te crystals was approximately 10 kg/mm^2 which is higher than the value of $\sim$8 kg/mm^2 in GaSe crystals.

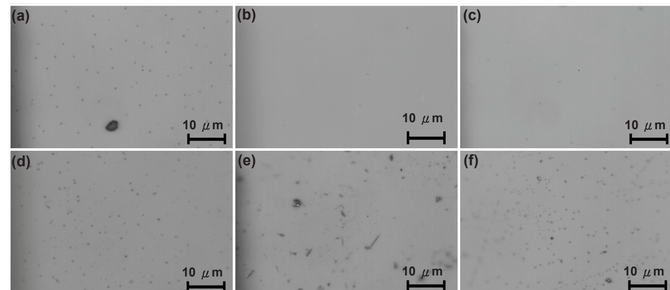

Fig. 1. Confocal microscopic images of (a) pure GaSe, (b) GaSe:Te (0.01 mass%), (c) GaSe:Te (0.07 mass%), (d) GaSe:Te (0.38 mass%), (e) GaSe:Te (0.67 mass%) and (f) GaSe:Te (2.07 mass%) crystals.

2.2. Optical properties

Mid-IR transmission spectra were recorded by FTIR VERTEX 70v (Bruker Optics Corp.) spectrometer with an operation wavelength range of 8000-375 cm^{-1} and spectral resolution of 0.16 cm^{-1}. Thickness of the GaSe sample examined in this measurement was of 0.89 mm. The thickness of the 0.01, 0.07, 0.38, 0.67, and 2.07 mass% Te-doped GaSe samples were 1.14, 1.00, 1.00, 0.98, and 0.87 mm, respectively. The typical mid-IR transmission spectra are presented in Fig. 2. The features with strong low-frequency absorption and the position of phonon mode in GaSe remain the same for Te doped GaSe. This implies that Te doping is unavailable for changing the optical quality in mid-IR range.

Mid-IR absorption coefficients were estimated from Fig. 2, and also determined in local point-to-point measurements by using low power CO_2 laser ($\emptyset\sim$1.0 mm) at 9.6 μm to minimize the influence of the microscopic surface and bulk defects on the measurement results. Subsequently, the point measurement data were applied to calibrate transmission spectra recorded by the mid-IR spectrophotometer. Because of the low mid-IR absorptivity, the presence of surface and bulk micro-defects, and the drifts of zero and 100% levels in spectra, we estimated only upper limit of the o-wave absorption coefficients and were unable to quantitatively characterize the optical quality as a function of doping levels in these six GaSe:Te crystals. The average absorption coefficients α in pure GaSe and GaSe:Te (0.01, 0.07, 0.38 mass%) crystals estimated from calibrated absorption spectra were within 0.1-0.2 cm^{-1}. For a 0.67 mass% GaSe:Te crystal, the average absorption coefficient was estimated as of 0.3-0.4 cm^{-1}, which can be reduced to 0.2 cm^{-1} by measuring the local point. However, because of the noticeable precipitates in a 2.07 mass% GaSe:Te crystal, as shown in Fig. 1(f), the higher absorption coefficients with a fluctuating range from $\leq$ 1 cm^{-1} to a few cm^{-1} were obtained in the local points. Moreover, the strongly anisotropic absorption ($\alpha_e > \alpha_o$) in GaSe crystals does not change in Te-doped

#157970 - $15.00 USD Received 10 Nov 2011; revised 16 Dec 2011; accepted 6 Jan 2012; published 14 Feb 2012
(C) 2012 OSA

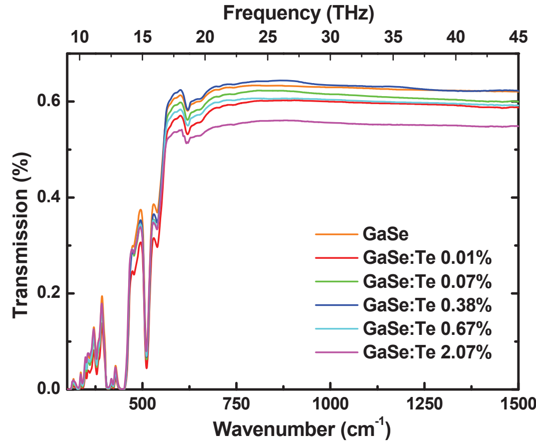

Fig. 2. IR transmission spectra of various Te-doped GaSe crystals.

GaSe crystals.

The optical properties in the range of 0.4-2.0 THz were measured by a home-made THz time-domain spectroscopy (TDS) system, as described elsewhere [16]. The THz pulses were generated by home-made biased $5\times5\times1$ mm InP photoconductive switch under the pumping of 50 fs pulses from Ti:sapphire laser (central wavelength: 800 nm, pulse repetition rate: 80 MHz). The generated THz pulses propagated through four off-axis parabolic mirrors and focused on a 1-mm-thick (110) ZnTe crystal, which was used to probe the THz pulse waveform by the free-space electro-optic (EO) sampling technique. The entire experimental setup was placed in an airtight enclosure purged with dry nitrogen and maintained at a relative humidity of < 3.0 % to avoid the strong absorption of the water vapor in THz range. In this study, THz beam was normally incident to the crystal surfaces.

It was necessary to consider the lattice vibration contribution to the free carriers to investigate complex dielectric function of GaSe:Te crystals in THz range. According to the combined Drude-Lorentz model, the total complex dielectric function $\tilde{\varepsilon}(\omega)$ [21] is given by

$$\tilde{\varepsilon}(\omega) = \varepsilon(\infty) + \sum_{j=1}^{J} \frac{S_j \omega_{TO_j}^2}{\omega_{TO_j}^2 - \omega^2 - i\Gamma_j \omega} - \frac{\omega_p^2}{\omega(\omega + i < \tau >^{-1})}, \tag{1}$$

where S_j is the strength of the oscillator, ω_{TO_j} is the frequency of the transverse optical phonon, Γ_j is the phonon relaxation rate, ω_p is the plasma frequency, and $< \tau >$ is the average momentum relaxation time for free carriers. The first term of right-hand side, $\varepsilon(\infty)$, is the high-frequency dielectric constant related to bound electrons; the second term describes the contribution of optical phonons; and the third term is the contribution from free electrons or plasmons. From the Drude-Lorentz model approximation, the complex dielectric function is given by the following equation:

$$\tilde{\varepsilon}(\omega) = (n(\omega) + i\kappa(\omega))^2 = \varepsilon(\infty) + \frac{i\hat{\sigma}}{\omega\varepsilon_0}, \tag{2}$$

where the complex conductivity $\hat{\sigma}(\omega)$ can be written as $\hat{\sigma}(\omega) = \sigma_r(\omega) + i\sigma_i(\omega)$. The real part of conductivity $\sigma_r(\omega) = 2n\kappa\omega\varepsilon_0(\kappa = c\alpha/2\omega)$ can be obtained from Eq. (1) and Eq. (2), as follows:

#157970 - $15.00 USD Received 10 Nov 2011; revised 16 Dec 2011; accepted 6 Jan 2012; published 14 Feb 2012
(C) 2012 OSA

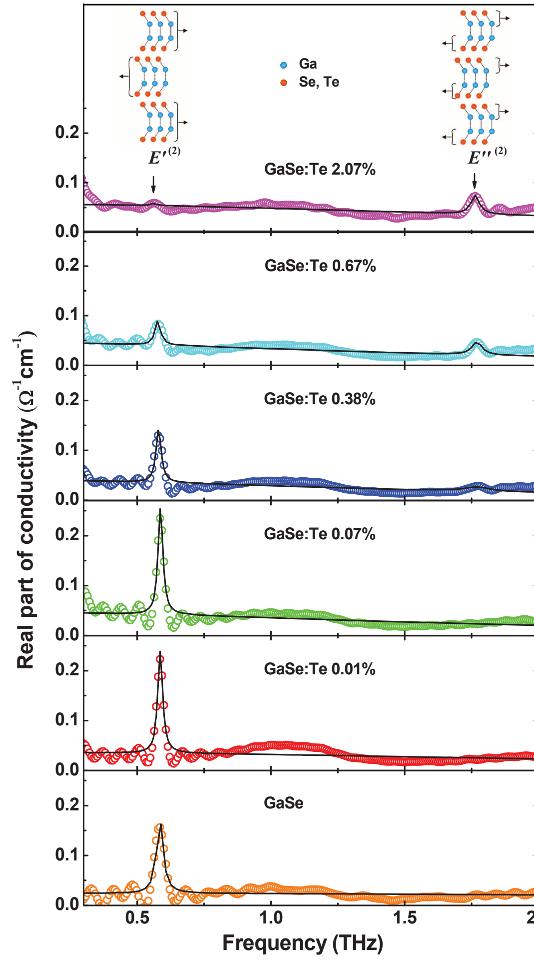

Fig. 3. O-wave real part of conductivity spectra in GaSe:Te crystals. Points: experimental data. Solid lines: fitting by Eq. (3). The inset in the upper figure shows the vibrational displacements of the rigid layer mode E'$^{(2)}$ and two-atom sub-layer mode E"$^{(2)}$ in a primitive layer.

$$\sigma_r(\omega) = \frac{\varepsilon_0 \omega_p^2 < \tau >^{-1}}{[\omega^2 + < \tau >^{-2}]} + \sum_{j=1}^{J} \frac{\varepsilon_0 S_j \Gamma_j \omega_{TO_j}^2 \omega^2}{(\omega_{TO_j}^2 - \omega^2)^2 + \Gamma_j^2 \omega^2}. \tag{3}$$

By using Eq. (3), we fit the experimental data of the real part conductivity (see Fig. 3) with the free-space permittivity of $\varepsilon_0 = 8.854 \times 10^{-12}$ F/m. All the fitting parameters are summarized in Table 1.

By theoretical fitting in Fig. 3, the absorption phonon modes can be described precisely by a number of physical parameters, as listed in Table 1. For instance, the oscillator strength S_j, an estimation of the intermolecular interaction, is Te-doping dependent in GaSe crystals and has a maximal value for 0.07 mass% GaSe:Te.

Because of the low absorptivity in the THz range, the presence of surface and bulk micro-defects, and the drifts of zero and 100% levels in spectra, we estimated only the upper limit of o-wave absorption coefficients, and were unable to quantitatively characterize the optical

#157970 - $15.00 USD Received 10 Nov 2011; revised 16 Dec 2011; accepted 6 Jan 2012; published 14 Feb 2012
(C) 2012 OSA

Table 1. Fitting parameters for Eq. (3).

Te concentration (mass%)	0	0.01	0.07	0.38	0.67	2.07
Phonon frequency ω_{TO_1} (THz)	0.584	0.586	0.587	0.580	0.577	0.564
Phonon relaxation rate Γ_1 (THz)	0.030	0.022	0.022	0.024	0.026	0.017
Oscillator strength S_1 (a.u.)	0.146	0.150	0.154	0.085	0.037	0.004
Phonon frequency ω_{TO_2} (THz)	-	-	-	1.77	1.77	1.76
Phonon relaxation rate Γ_2 (THz)	-	-	-	0.121	0.046	0.038
Oscillator strength S_2 (a.u.)	-	-	-	0.0037	0.0043	0.0050

quality as a function of doping levels in these six GaSe:Te crystals and identify the optimal doping level. The average absorption coefficients in THz range were <5 cm^{-1} of GaSe:Te with 0, 0.01, 0.07, and 0.38 mass%. Furthermore, the higher absorption coefficients of 7.7 cm^{-1} and $\geq$9.7 cm^{-1} were obtained from 0.67 and 2.07 mass% GaSe:Te crystals, respectively.

2.3. THz generation via optical rectification

In this section, we describe THz generation in pure and Te-doped GaSe crystals through the optical rectification method by a commercial Ti:sapphire oscillator with a pulse duration of $\sim$70 fs and repetition rate of 5.2 MHz. By using a 100-μm-thick (110)-oriented ZnTe crystal as EO detector, the temporal waveforms of the THz field from GaSe:Te crystals were measured using the EO sampling technique, as shown in Fig. 4(a).

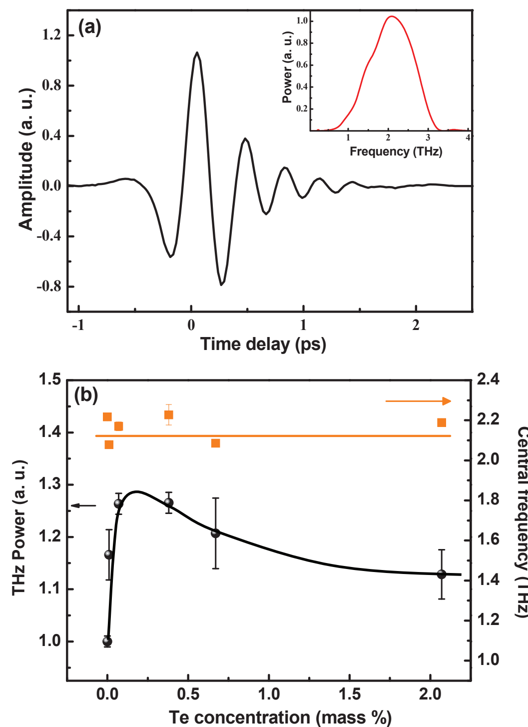

Fig. 4. (a) Temporal waveform of THz radiation on a 0.30-mm GaSe:Te (0.07 mass%) crystal. The inset illustrates the power spectra from the fast Fourier transform of the temporal waveform. (b) The central frequency and the THz generation power at various Te concentrations.

#157970 - $15.00 USD Received 10 Nov 2011; revised 16 Dec 2011; accepted 6 Jan 2012; published 14 Feb 2012
(C) 2012 OSA

All specimens were fabricated with an almost fixed thickness (approximately 0.3 mm) to compare the THz generation efficiency. The fast Fourier transformation (FFT) of the temporal profile of THz pulse was used to obtain the central frequency and output power of THz radiation, as illustrated in the inset of Fig. 4(a). Consequently, the power and the central frequency of the generated THz pulses on all GaSe:Te crystals were extracted, as shown in Fig. 4(b). The central frequency of THz emission was independent of the Te-doping in GaSe crystals. However, the Te dopant in GaSe crystals considerably improved the THz output power. The highest conversion efficiency, over 20% higher than that of a pure GaSe crystal, was found in a 0.07 mass% Te-doped GaSe crystal.

3. Discussion

Crystals grown from the charge compositions of GaSe with nominal 0.05, 0.1, 0.5, 1, and 3 mass% of Te were identified as the noncentrosymmetric ε-GaSe:Te (0.01, 0.07, 0.38, 0.67, and 2.07 mass%) crystals, which are useful for non-linear applications. The crystal structure of the heavy Te-doped (nominal 5 and 10 mass%) GaSe crystals were polycrystalline, and unsuitable for non-linear applications. A small 0.02-THz shift of the central frequency of the phonon mode $E'^{(2)}$ (in Table 1) was observed only in GaSe:Te with 2.07 mass% crystals. This indicates that the slight doping of Te has almost no influence on the lattice parameters of GaSe crystals. The low absorptivity in slightly Te-doped GaSe limited us to resolve the small changes of the absorption coefficients in THz and mid-IR ranges with maximal transparency, as well as to identify optimal Te-doping in GaSe crystals.

Furthermore, the noticeable changes in the absorption peak intensities of the phonon modes $E'^{(2)}$ and $E''^{(2)}$ were observed with various Te dopings, as shown in Fig. 3. For $E'^{(2)}$ at $\sim$0.584 THz, the so-called rigid layer mode was formed because the GaSe layers vibrated as rigid units and no relative displacement occurred between the Ga and Se atoms within a basic layer, as illustrated in the inset of Fig. 3. However, if the layers vibrate with the relative displacement between two Ga-Se sub-layers within four-atom rigid layers (see the inset of Fig. 3), the frequency of phonon mode would be higher than the rigid layer mode, that is, the $E''^{(2)}$ mode at 1.77 THz, as shown in Fig. 3 [22]. First, we focused on the intensity evolution of absorption peaks as increasing the concentration of Te. For slight Te-doping, the absorption peak of the rigid layer mode $E'^{(2)}$ gradually increased until it reached maximal value at Te-doping of 0.07 mass%. This indicates that the lattice structure in GaSe was improved by decreasing the number of point- and layer-stacking defects with Te-doping [8, 23], which correlates with the clear images in Figs. 1(b) and 1(c), respectively. Consequently, the optical quality of GaSe:Te was also considerably improved by Te-doping. However, the shrink of the absorption peak of the rigid layer mode $E'^{(2)}$ reveals that the improvement of the lattice structure and optical quality in GaSe cannot be further extended by more Te dopings. This degradation of optical quality in Te-doped GaSe crystals can be caused by increasing structural defects (polytypism, stacking faults, dislocations) [20, 23, 24], defect complexes [13, 24], exciton-phonon and exciton-impurity interactions [25], intensive interlayer (interstitial) species [23, 26], and formation of strained regions [25]. For heavy Te-doped GaSe crystals, the rigid layer mode $E'^{(2)}$ disappears, which is consistent with the results of [20] and the observations in GaSe:S crystals [16]. As the rigid layer mode $E'^{(2)}$ shrink, the phonon mode $E''^{(2)}$ at 1.77 THz, which was also observed in GaSe:S crystals [16],gradually increased in intensity in conjunction with the Te dopings. No distinct reason was found to explain the increase of $E''^{(2)}$ mode; however, interlayer intercalation of larger-size Te atoms [13, 25] led to the formation of the local strained regions that bond hard Se-Ga sub-layers.

The results of the THz pulse generation in GaSe:Te (0, 0.01, 0.07, 0.38, 0.67 and 2.07 mass%) through optical rectification in Fig. 4 reveal the strong correlation between the intensity of the

#157970 - $15.00 USD Received 10 Nov 2011; revised 16 Dec 2011; accepted 6 Jan 2012; published 14 Feb 2012
(C) 2012 OSA

absorption peak of phonon mode E'$^{(2)}$ and THz generation efficiency, that is, the optical quality in Te-doped GaSe crystals. The THz generation efficiency in 0.07 mass% GaSe:Te crystals was over 20% higher than that in pure GaSe crystals. Further improvement in the generation efficiency is possible by carefully tuning the Te-doping level between 0.07 and 0.38 mass%, optimizing the crystal length because of the so-called "scaling up" effect [8], and improving surface quality. It is also proposed that the higher damage threshold can be reached due to higher optical quality in optimally doped GaSe crystals if the surface defects can be suppressed to allow higher pump intensity.

Because of a narrow window for the optimal concentration of Te doping in GaSe crystals, which were not considered or occasionally omitted, no optimally Te-doped GaSe have been reported in previous studies. However, the optimal doping in GaSe crystals is crucial in the application of sub-cm and cm-sized crystals in long-pulse frequency conversion at mid-IR and down-conversion into THz range [15] as it proceeds from the "scaling up" effect [8]. This study is the first to demonstrate the evolution of E'$^{(2)}$ and E"$^{(2)}$ phonon modes measured by THz TDS to identify the optical quality and the optimal doping levels in doped GaSe crystals.

4. Conclusion

Centimeter-sized Te-doped GaSe ingots were grown from the charge compositions of GaSe with nominal 0.05, 0.1, 0.5, 1, and 3 mass% of Te, which were identified as ε-GaSe:Te (0.01, 0.07, 0.38, 0.67, and 2.07 mass%) single crystals and suitable for non-linear applications. We found a strong correlation between intensity of the rigid layer mode E'$^{(2)}$ at $\sim$0.584 THz and the optical quality in Te-doped GaSe crystals. This study was the first to use this correlation as a sensitive mean for determining the optical quality in doped GaSe, and as an efficient tool for determining the optimal doping level. This was further confirmed by the THz generation experiments. The Te doping of approximately 0.07 mass% was identified as the optimal doping for THz generation through optical rectification, resulting in 20% improvement in generation efficiency. Further improvement in the efficiency can be achieved by fine-tuning the doping levels and the crystal length because of so-called "scaling up" effect, by canceling the surface defects and increasing pump intensity.

Acknowledgments

This work is supported by the National Science Council of Taiwan, R.O.C. under grant: NSC96-2923-M-009-001-MY3, NSC98-2112-M-009-008-MY3, and by the Grant MOE ATU Program at NCTU and RFBR Project No.10-02-01452-a, Presidium SB RAS under the Project VII.63.3.1 of VII.63.3 Prog. and Joint Proj. between Presidium SB RAS and Presidium NAS, Belarus No.10 of 2010.

#157970 - $15.00 USD Received 10 Nov 2011; revised 16 Dec 2011; accepted 6 Jan 2012; published 14 Feb 2012
(C) 2012 OSA